Applied Physics Letters PERSPECTIVE scitation.org/journal/apl

A perspective on curvilinear magnetism

Cite as: Appl. Phys. Lett. **118**, 230502 (2021); doi: 10.1063/5.0048891
Submitted: 27 February 2021 · Accepted: 8 May 2021 ·
Published Online: 10 June 2021

View Online Export Citation CrossMark

Denis D. Sheka[a]

AFFILIATIONS

Taras Shevchenko National University of Kyiv, 01601 Kyiv, Ukraine

Note: This paper is part of the APL Special Collection on Mesoscopic Magnetic Systems: From Fundamental Properties to Devices.
[a]**Author to whom correspondence should be addressed:** sheka@knu.ua

ABSTRACT

By exploring geometry-governed magnetic interactions, curvilinear magnetism offers a number of intriguing effects in curved magnetic wires and curved magnetic films. Recent advances in experimental techniques change the status of curvilinear magnetism, allowing the exploitation of 3D curved nanomagnets in emerging devices with numerous applications. Here, we provide our Perspective on the recent progress, challenges, and prospects of curvilinear magnetism with a special focus on novel physical effects caused by tailoring curvature and topology of conventional magnetic materials.

Published under an exclusive license by AIP Publishing. https://doi.org/10.1063/5.0048891

I. INTRODUCTION

Recent advances in nanotechnologies have enabled fabrication of the novel class of 3D curved magnetic nanoarchitectures,[1] where the fundamental properties are determined by the geometry.[2] Active exploration of this new material class turns light on the fundamentals of magnetism of nanoobjects with curved geometry and applications of 3D-shaped curved magnetic nanoarchitectures, leading to remarkable developments in shapable magnetoelectronics,[3,4] magnetic sensorics,[5] spintronics,[2,6] 3D magnonics,[7] and microrobotics.[8,9] Today, fundamental and applied research of curved nanoarchitectures and related curvature-induced effects in these objects are united in *curvilinear magnetism*, which is a rapidly developing research area of modern magnetism aimed to explore geometry-induced effects in curved magnetic wires and films.[10] Different aspects of magnetism in curved geometries and 3D nanomagnetism are comprehensively elaborated in review articles.[2,6,11]

By extending planar geometries into 3D space, there appear new, sometimes unexpected, physical effects stemming from a mutual interplay between the geometrical properties of the underlying substrate and the magnetic order parameter. The dominant reasons for this can be ascribed to the geometry-governed emergent magnetic interactions caused by local and global geometric aspects: emergent anisotropy and emergent chiral interaction with the Dzyaloshinskii–Moriya interaction is a key example.[2] Following a brief introduction to methods of synthesis curved magnets and imaging techniques, this Perspective then primarily focuses on emergent interactions and physical effects caused by geometrically curved magnetic wires and films. By reviewing topological patterning and geometrical magnetochiral effects, we highlight prospect directions of fundamental and applied research in the field of curvilinear magnetism.

II. FABRICATION AND CHARACTERIZATION

It is a peculiarity of curvilinear magnetic nano-architectures to keep a balance between low dimensionality of nanomagnetism and the 3D design to achieve new features of the curved geometry. This is granted, first of all, by recent advances in experimental techniques. Here, we briefly mention fabrication methods used to synthesize curved magnets.

Typically, curvilinear flat architectures are fabricated using conventional techniques based on thin film deposition and lithographic methods, which are widely used to fabricate planar curved nanowires and stripes[12–16] and nanorings.[17–19] Flat spiral structures [Fig. 1(f)] can be patterned using ion-beam writing.[20,21] Fabrication of complex-shaped 3D nanoarchitectures is challenging, and it becomes enabled by the advent of techniques. Glancing angle deposition (GLAD) is a conventional technique for fabrication of individual nanohelices [Fig. 1(a)],[22] an array of sculpted 3D objects such as helices, posts, and chevrons.[23] Strain-engineering technologies[3,4] allow to develop novel materials, including a variety of rolled-up and wrinkled magnetic nanomembranes[2] such as microhelix coil structures,[24] Swiss rolls,[25] and complex micro-origami structures.[26] Different chemical synthesis techniques include self-assembly, combinations of 3D templates usage with electroless and atomic layer deposition, and electroplating; this allows to fabricate core–shell nanowires,[27] multilayered nanotubes,[28] core/shell nanoparticles,[29] and hollow nanoparticles.[30] Special activity is dedicated to magnetic nanocap structures, which allows to create

Published under an exclusive license by AIP Publishing

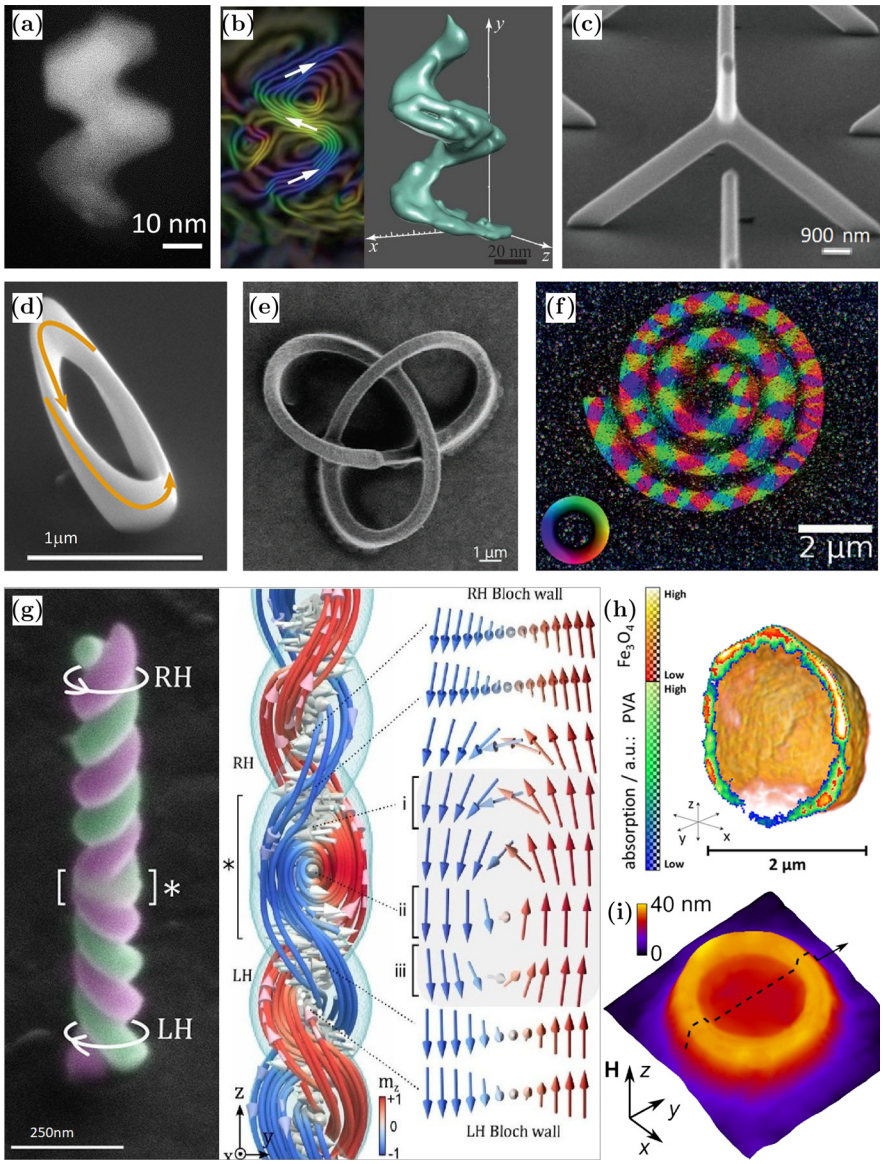

FIG. 1. Fabrication and visualization of curved nanostructures. (a) Imaging by high-angle annular dark-field scanning transmission electron microscopy of Co nanohelix produced using the GLAD technique: adapted with permission from Gibbs *et al.*, Nanoscale **6**, 9457 (2014).[22] Copyright 2014 Royal Society of Chemistry. (b) Electron holography image of the magnetization texture in Co nanohelix produced using the GLAD technique: adapted with permission from Phatak *et al.*, Nano Lett. **14**, 759 (2014).[47] Copyright 2014 American Chemical Society. (c) SEM image of a 3D tetrapod structure fabricated using two-photon lithography: reproduced with permission from Williams *et al.*, Nano Res. **11**, 845–854 2018.[32] Copyright 2018 Authors, licensed under a Creative Commons Attribution 4.0 International License. (d) SEM image of a cobalt Möbius strip fabricated by FEBID: adapted with permission from Skoric *et al.*, Nano Lett. **20**, 184 (2020).[45] Copyright 2020 Authors, licensed under a Creative Commons CC-BY agreement. (e) Ni–Fe trefoil-knots by electroless deposition on a 3D-printed polymer scaffold: reproduced with permission from Pip *et al.*, Small **16**, 2004099 (2020).[34] Copyright 2020 John Wiley and Sons. (f) STEM-DPC image of the spiral structure fabricated by ion-induced methods: reproduced with permission from Nord *et al.*, Small **15**, 1904738 (2019).[20] Copyright 2019 Authors, licensed under a Creative Commons CC-BY license. (g) SEM image of the cobalt nanostructure consisting of two double-helices of opposite chirality joined at the tendril perversion marked with $*$, fabricated by FEBID: adapted with permission from Sanz-Hernández *et al.*, ACS Nano 14, 8084 (2020).[43] Copyright 2020 Authors, licensed under a Creative Commons CC-BY license. (h) Soft x-ray laminography of PVA microsphere coated with magnetite nanoagglomerates: reproduced with permission from Witte *et al.*, Nano Lett. **20**, 1305–1314 (2020).[57] Copyright 2020 American Chemical Society. (i) AFM image of Co_3Fe nanovolcano fabricated by FEBID: reproduced with permission from Dobrovolskiy *et al.*, Appl. Phys. Lett. **118**, 132405 (2021).[46] Copyright 2021 AIP Publishing LLC.

isolated hemispherical and cylindrical caps as well as cap arrays, caps with different anisotropy orientations; such cap structures host vortices, skyrmions, and more complex spin textures. Nanocap structures and their application for magnetic data storage as well as for life sciences are reviewed in Ref. 2. A recent development of two-photon lithography combined with different metalization techniques allows to fabricate rapidly complex 3D nanostructures with examples of a tetrapod individual structure and their array,[31–33] a buckyball structure,

Published under an exclusive license by AIP Publishing

and trefoil-knots [Fig. 1(e)].[34] Interconnected nanowire networks have been achieved recently using electrodeposition into polycarbonate membranes.[35] The most extensive flexibility to fabricate complex-shaped 3D nano-architectures without limitations of specific geometries is provided today by a direct-write *3D nanoprinting*, which is a collective name of different techniques involving beam or optical deposition on scaffolds or direct growth of magnetic materials. Amid different nanoprinting techniques, the focused electron beam induced deposition (FEBID)[36–38] enables to pattern complex 3D magnetic nanostructures at resolutions comparable to the characteristic magnetic length scales.[39] FEBID nanoprinting is used to fabricate complex 3D nanowires including nanospirals,[40] nanobridges,[41] nanohelices,[42] double-helices [Fig. 1(g)],[43] artificial structures like tetrapods, tetrahedra,[39] nanotrees, nanocubes, and their lattices,[44] and exotic 3D object with curved magnetic surfaces such as Möbius nanorings [Fig. 1(d)][45] and nanovolcanoes [Fig. 1(i)].[39,46]

Curvilinear magnetism requires advanced imaging techniques since 3D-shaped nanoobjects can hide substantial parts of their structure for conventional top-view imaging. Besides, 3D structural and magnetic properties of 3D nanoobjects are typically caused by a complex 3D coordinate dependence of the magnetization fields, which may only be revealed with full vector-field tomographic reconstructions. High-resolution characterization of curved 3D magnets is achieved by techniques such as Lorentz transmission electron microscopy [Fig. 1(b)],[47] dark-field MOKE magnetometry,[48] Brillouin light scattering [Fig. 4(d3)],[7,49] electron holography,[50] NV magnetometry,[51,52] vector field electron tomography,[42,53,54] hard-x-ray vector nanotomography,[55] soft-x-ray tomography,[56] and soft x-ray laminography [Fig. 1(h)],[57] for review see Refs. 2, 6, and 11.

Thriving fabrication and characterization techniques of curvilinear magnets provide a wide testing area for fundamental research of novel effects induced by geometrically curved materials. Besides, these techniques allow exploiting 3D nano-architectures in novel devices with prospective applications.

III. EMERGENT INTERACTIONS AND CURVATURE-INDUCED EFFECTS

By tailoring *curvature* and *topology* of conventional magnetic materials, there appears a possibility to control material response leading to modification or even launching new functionalities.[2,6,11] All these new material properties became a reality due to curvature-induced effects, which are originated from the *geometry-governed* magnetic interactions. Various geometrical aspects of the underlying substrate affect the magnetic subsystem in different ways. In particular, local geometric properties like local curvatures are crucial for understanding the local magnetic interactions in curved magnets, in particular, exchange interaction, magneto-crystalline anisotropy, and Dzyaloshinskii–Moriya interaction (DMI). Global geometric aspects are essential, first of all, for nonlocal magnetic interactions such as a magnetostatic interaction. Among different global geometric aspects, one has to mention geometric confinement: it is important for the magnetic texture patterning, but it has no direct connection to the curvilinear magnetism. Topology, as another global geometric aspect, can be decisive for the pattern formation in curved magnets.

There are two principal sources of the geometry-governed magnetic interactions: (i) The magneto-crystalline anisotropy direction $\boldsymbol{e}_\mathrm{a}$ in curved magnets is determined by a spatial variation of the anisotropy axis $\boldsymbol{e}_\mathrm{a} = \boldsymbol{e}_\mathrm{a}(\boldsymbol{r})$, which follows the sample geometry;[24,58,59] and (ii) the magnetostatic interaction in thin curved nanoobjects induces the shape anisotropy with axis $\boldsymbol{e}_\mathrm{a}$ following the sample geometry, similar to the magneto-crystalline anisotropy. Such a reduction of the nonlocal interaction to the local anisotropy was rigorously derived for curved wires,[60] shells,[61,62] and films.[63]

A unifying description of the curvature-induced effects is based on a micromagnetic framework of curvilinear magnetism,[64] which allows to treat local and nonlocal interactions on equal footing. Let us focus on a classical uniaxial ferromagnet with the following energy density:

$$\mathscr{E} = \mathscr{E}^\mathrm{x} + \mathscr{E}^\mathrm{A} + \mathscr{E}^\mathrm{DMI} + \mathscr{E}^\mathrm{MS}. \tag{1}$$

Here, $\mathscr{E}^\mathrm{x} = -A\boldsymbol{m}\cdot\boldsymbol{\nabla}^2\boldsymbol{m}$ is the exchange energy density with A being the exchange constant, $\boldsymbol{m} = \boldsymbol{M}/M_\mathrm{s}$ being the normalized magnetization, and M_s being the saturation magnetization; the anisotropy energy density $\mathscr{E}^\mathrm{A} = K(\boldsymbol{m}\cdot\boldsymbol{e}_\mathrm{a})^2$ with K being the anisotropy constant and $\boldsymbol{e}_\mathrm{a}$ being the anisotropy axis; the DMI energy density $\mathscr{E}^\mathrm{DMI} = D\sum_{ijk}\mathscr{L}_\mathrm{ij}^{(\mathrm{k})}$ is composed of Lifshitz invariants $\mathscr{L}_\mathrm{ij}^{(\mathrm{k})} = \mathrm{m_i}\partial_\mathrm{k}\mathrm{m_j} - \mathrm{m_j}\partial_\mathrm{k}\mathrm{m_i}$ with D being the DMI constant; and the magnetostatic energy density $\mathscr{E}^\mathrm{MS} = \frac{1}{2}M_\mathrm{s}^2\int_V \mathrm{d}\boldsymbol{r}'(\boldsymbol{m}(\boldsymbol{r})\cdot\boldsymbol{\nabla})(\boldsymbol{m}(\boldsymbol{r}')\cdot\boldsymbol{\nabla}')|\boldsymbol{r}-\boldsymbol{r}'|^{-1}$.

The key idea of the corresponding theory is to represent the magnetic subsystem in a curvilinear reference frame, which follows the sample geometry (one of the curvilinear basis vectors is determined by $\boldsymbol{e}_\mathrm{a}$), providing means to recover the translation invariance of the effective anisotropy.[70] The usage of specific curvilinear frames adopted to the geometry allows to systematize geometrical effects by restructuring all magnetic energy terms according to their local spatial symmetry[64]

$$\mathscr{E} = E_0 + \underbrace{E_\mathrm{A}}_{\substack{\text{effective}\\ \text{anisotropy}}} + \underbrace{E_\mathrm{D}}_{\substack{\text{mesoscale}\\ \text{DMI}}} + \underbrace{E_\mathrm{MS}}_{\substack{\text{magneto-}\\ \text{statics}}}. \tag{2}$$

The applicability of the current micromagnetic framework requires that the sample has a constant thickness h along the normal, and the anisotropy directions $\boldsymbol{e}_\mathrm{a}$ do not vary along the thickness. This makes it possible to suppose that the magnetization texture remains uniform along the direction of the normal to the sample,[64] which typically means that the sample thickness does not exceed several times the characteristic magnetic length scale ℓ. One more restriction is that h should be much smaller than that of the typical curvature radii $\mathscr{R}$.[70,71] These limitations specify the applicability of the theory to the description of quasi-1D and quasi-2D objects in the case of curved wires and films, respectively. This means that the existing theory is not suitable for the description of 3D topological defects such as Bloch points, chiral bobbers, and hopfions.[72]

The first energy contribution E_0 in (2) absorbs terms that do not depend explicitly on the curvature of the system and can result in chiral effects even in a purely planar case due to the chiral magnetic texture, the so-called pattern-induced chirality breaking.[2] The second term, an effective anisotropy, E_A comprises the intrinsic magneto-crystalline anisotropy $\mathscr{E}^\mathrm{A}$ and extrinsic curvilinear geometry-governed contributions, which take, in general, the form of biaxial anisotropy, $\mathscr{K}_{\alpha\beta}m_\alpha m_\beta$ (here and below Greek indices α, β, and γ numerate curvilinear coordinates and curvilinear components of magnetization). There are two major sources of this extrinsic anisotropy. One of them is driven by exchange. For curved films, components of $\mathscr{K}_{\alpha\beta}$ have a bilinear form with respect to principle curvatures κ_1 and κ_2 of the

Published under an exclusive license by AIP Publishing

surface, $\|\mathscr{K}_{\alpha\beta}\| = A\mathrm{diag}(\kappa_1^2; \kappa_2^2; \kappa_1^2 + \kappa_2^2)$.[64] The anisotropy coefficients have a bilinear form with respect to the wire curvature κ and its torsion τ for curved wires; $\mathscr{K}_{\alpha\beta} = \mathscr{F}_{\alpha\gamma}\mathscr{F}_{\beta\gamma}$ with $\mathscr{F}_{\alpha\beta}$ being the Frenet–Serret tensor determined by κ and τ.[71] Another source of the geometry-induced anisotropy is driven by DMI. In the case of curved films and the interfacial type of DMI, $\|\mathscr{K}_{\alpha\beta}\| = -D\mathscr{H}\mathrm{diag}(0; 0; 1)$[73] with $\mathscr{H} = \kappa_1 + \kappa_2$ being the mean curvature of the film surface; for curved wires $\mathscr{K}_{\alpha\beta}$ is linear with respect to κ and τ.[74]

An effective DMI term E_{D} adsorbs two contributions: An intrinsic DMI in the curved geometry, $D\sum_{\alpha\beta\gamma}\mathscr{L}^{(\gamma)}_{\alpha\beta}$, is determined by the curvilinear-geometry analogue of Lifshitz invariants $\mathscr{L}^{(\gamma)}_{\alpha\beta} = m_\alpha\eth_\gamma m_\beta - m_\beta\eth_\gamma m_\alpha$. Here, $\eth_\alpha$ is the tangential derivative that naturally appears for the description of the curved films;[64] in the case of a curved wire, the energy depends only on invariants of the form $\mathscr{L}^{(s)}_{\alpha\beta} = m_\alpha\partial_s m_\beta - m_\beta\partial_s m_\alpha$ with s being the coordinate along the wire.[74] A curvature-induced exchange-driven extrinsic DMI has similar structure as intrinsic one. For the curved films, the corresponding DMI energy density is linear with respect to principal curvatures, $2A\kappa_\alpha\mathscr{L}^{(\alpha)}_{\alpha n}$.[64] The DMI energy density of curved wires $2A\mathscr{F}_{\alpha\beta}\mathscr{L}^{(s)}_{\alpha\beta}$ is linear with respect to curvature and torsion.[71] Two different types of DMI, intrinsic and extrinsic, influence only inhomogeneous magnetic textures acting at different lengthscales. That is why the resulting effective DMI is referred to as *mesoscale DMI*.[74] It is important that the symmetry and amplitude of the resulting DMI are determined by both material and geometrical properties, offering possibilities to tune both magnitude and directions of the mesoscale DMI by geometrical manipulations.[74]

The last term in (2) is the magnetostatic interaction. Unlike all other interactions, the magnetostatic contribution is essentially nonlocal. To understand its symmetry in curved wires and curved films, it is instructive to go beyond the well-established picture of volume and surface magnetostatic charges by involving three fictitious mathematical constructions in the description, which are locally sensitive to the curved geometry:[64] A surface charge σ is determined by the normal component of magnetization. A tangential charge ρ is determined by its tangential components: $\rho = -\eth_\alpha m_\alpha$ for curved films and $\rho = -\partial_s m_{\mathrm{T}}$ for curved wires with m_{T} being the tangential magnetization component along the wire. The most intriguing term is the geometrical charge g, which represents the coupling between the magnetization texture and the geometrical curvature. For curved films, $g = \mathscr{H}m_N$,[64] and for curved wires, $g = \kappa m_{\mathrm{N}}$ with m_{N} being the normal magnetization component. Usage of these three charges allows restructuring the magnetostatic interaction adapted to the curved geometry

$$E_{\mathrm{MS}} = E_{g-\sigma} + E_{g-g} + E_{g-\rho} + E_{\sigma-\rho}, \tag{3}$$

where each term E_{a-b} describes the pair interaction between two charges of type "a" and "b," an explicit form see Ref. 64. Similar energy restructuring was performed previously for particular cases of tubular[75] and spherical[66] shells.

During several years after its theoretical prediction, novel geometry-govern interactions were investigated only theoretically and checked numerically by means of micromagnetic and spin-lattice simulations. The first experimental confirmation of the existence of the curvature-induced local chiral interaction (DMI) driven by exchange has been performed recently by measuring the depinning field of domain walls in a flat parabolic stripe:[16] remarkably that experimentally quantified value of emergent DMI can be as high as the interfacial DMI constant for thin films. Very recently, the nonlocal chiral interaction driven by magnetostatics was directly observed experimentally by measuring the spin-wave propagation in magnetic nanotubes using TR-STXM measurements.[76]

Emergent interactions, induced by the curvilinear geometry, manifest themselves in topological magnetization patterning and magnetochiral effects in conventional magnetic materials.

A. Topological patterning

Geometry-governed emergent anisotropy and emergent DMI become the source of an effective curvature-induced magnetic field.[70,71] Originating from the mutual interplay between the symmetry of magnetic interactions, curvature, and magnetic texture, the effective field influences even the ground state magnetization: an assumed ground state becomes a subject of further modifications due to curvilinear effects.[64,70,71] For example, an emergent biaxial anisotropy in a helix nanowire causes the tilt of the ground state magnetization in the local rectifying surface[77] and an emergent DMI in curved nanoshells selects the winding numbers of merons.[78] In dynamics, the emergent biaxial anisotropy becomes the source of the Walker limit of the current-induced dynamics of domain walls in uniaxial circular-shaped wires.[79] Effective anisotropy is responsible for the shift of the magnon gap in the magnon dispersion law in nanotubes.[80]

An interplay between local and global geometrical aspects is supported by the nonlocal magnetostatic interaction. A striking manifestation of this interplay is the *topological patterning* (Fig. 2), i.e., the formation of topologically protected magnetization textures (topological magnetic solitons like domain walls, skyrmions, merons, etc.[72]) in topologically non-trivial curved geometries. A characteristic example is provided by a spherical shell, which corresponds to core–shell nanoparticles.[29] The geometry of a spherical shell prohibits an existence of uniform magnetization texture, even in the case of small spheres.[66] Instead, the texture with two topological defects is realized in the case of in-surface anisotropy: the 3D onion state [Fig. 2(c)] in the case of thin shells[81] or the whirligig state [Fig. 2(d)] in the case of thick shells.[66] In the case of perpendicularly magnetized spherical shell (normal anisotropy), the hedgehog magnetic texture becomes preferable.[73] A tubular geometry supports different topological states in magnetic nanotubes like vortex states, vortex [Fig. 2(a)] and transverse [Fig. 2(b)] domain walls in the case of axial domains,[65,75] Néel, Bloch, and cross-tie domain walls in the case of azimuthal domains,[82] and Bloch-point domain walls.[83] The symmetry of a hyperboloid shell favors vortex [Fig. 2(g)] and skyrmion [Fig. 2(h)] textures.[68] Toroidal [Fig. 2(e)] and poloidal [Fig. 2(f)] vortices are realized in toroidal shells[67] as well as more complex state consisting of vortex-antivortex pair.[84] A topology of nonorientable Möbius ring hosts different topologically protected domain walls [Figs. 2(i) and 2(j)].[69]

B. Geometrical magnetochiral effects

The curved geometry introduces a break in the spatial inversion symmetry, which is a source of emergent chiral interactions: (i) a local chiral interaction, i.e., DMI, driven by exchange[70] and (ii) a nonlocal chiral interaction driven by magnetostatics.[64] Both chiral interactions are responsible for *geometrical magnetochiral effects*, which represent chiral dependent magnetic textures governed by the curved geometry.

Published under an exclusive license by AIP Publishing

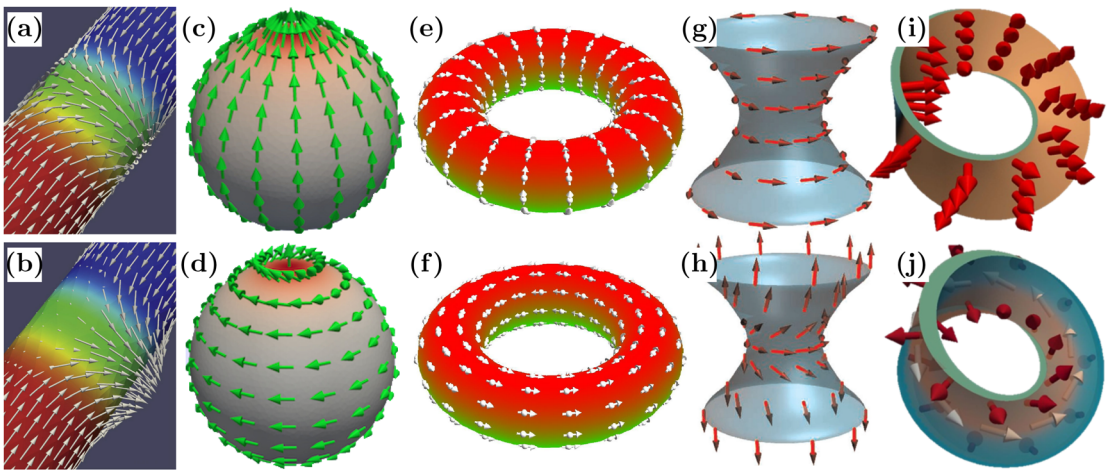

FIG. 2. Topological patterning corresponds to the formation of topologically protected magnetization textures in topologically non-trivial curved geometries. Characteristic examples include (a) vortex and (b) transverse domain walls in a nanotube: adapted with permission from López-López *et al.*, J. Magn. Magn. Mater. **324**, 2024 (2012).[65] Copyright 2012 Elsevier. (c) 3D onion and (d) whirligig states in spherical nanoshell: adapted with permission from Sloika *et al.*, J. Magn. Magn. Mater. **443**, 404 (2017).[66] Copyright 2017 Elsevier. (e) Toroidal and (f) poloidal vortices in a toroidal nanoshell: reproduced with permission from Teixeira *et al.*, J. Magn. Magn. Mater. **478**, 253–259 (2019).[67] Copyright 2019 Elsevier. (g) Vortex and (h) skyrmion patterns in hyperboloid: reproduced with permission from Carvalho-Santos *et al.*, J. Magn. Magn. Mater. **391,** 179–183 (2015).[68] Copyright 2015 Elsevier. (i) Transversal and (j) longitudinal domain walls in Möbius ring: reproduced with permission from Pylypovskyi *et al.*, Phys. Rev. Lett. **114**, 197204 (2015).[69] Copyright 2015 Authors, licensed under a Creative Commons Attribution 3.0 License.

There are numerous examples of chiral magnetic textures, including right-handed/left-handed Bloch domain walls,[98] clockwise/counterclockwise vortices,[99] Bloch skyrmions,[100] etc. Typically, all these textures are degenerated with respect to chiralities in flat geometries. Bending of the magnet breaks some of spacial symmetries. Nevertheless, the symmetry of the curved system can be still so high that the bending does not break the degeneracy with respect to opposite chiralities. This corresponds to *pattern-induced chirality breaking* (Fig. 3):[2] the chiral symmetry breaking occurs dynamically on the background of chiral-degenerated static magnetization texture. A paradigmatic example is a magnetic nanotube, where static vortex states[101] and vortex domain walls[75] are degenerated with respect to chirality. Nevertheless, these degenerated chiral magnetic patterns can serve as a springboard for magnon chiral effects: the splitting of magnons with left- and right handed chiralities on the background of the chiral vortex state[102,103] is driven by the pair interaction between different types of magnetostatic charges.[64] The curvature-induced asymmetric spin-wave dispersion was recently observed in magnetic nanotubes with hexagonal cross section using time resolved scanning transmission x-ray microscopy [Figs. 3(c) and 3(d)].[76] The chiral symmetry breaking for another chiral pattern, the vortex domain wall,[75] can support a chiral breakdown [Figs. 3(a)–3(c)],[85,104–106] trigger a Cherenkov-type spin-wave radiation,[107,108] and suppress the Walker breakdown.[109]

An intriguing graphic evidence of the magnetochiral effect provides a *geometry-induced chirality breaking* (Fig. 4), where the geometry-governed chiral interactions can realize an interplay between the geometrical chirality of the object and the magnetochirality[106] of the texture. The emergent DMI in helix wires provides the charge dependent domain wall handedness [Fig. 4(a4)].[79] In helicoid ribbons, the emergent DMI selects the preferable magnetization handedness of the ground state [Fig. 4(a3)].[86] Intrinsically, achiral one-dimensional curvilinear antiferromagnets behave as a chiral helimagnets with geometrically tunable DMI.[97] Representative consequences of the coupling between the geometrical helix chirality and the magnetic chirality are the nonreciprocity of the spin-wave spectrum,[77] the chirality sensitive domain wall mobility [Fig. 4(c2)],[90] and a negative mobility of the spin-torque driven domain wall.[79] Geometry-induced DMI becomes a source of spin wave mode hybridization in curvilinear antiferromagnets [Fig. 4(d5)].[97] Due to the geometry-induced chirality symmetry breaking, the magnetochirality of the domain walls in Möbius rings is determined by the geometrical chirality of the ring.[69]

Chiral interactions are known[98] to select handedness for achiral textures. That is why curvature-induced DMI shows itself even in curved flat magnetic systems providing the phase-selected pinning of domain walls in flat parabolic stripes;[110] the strength of emergent DMI is quantified experimentally by measuring the depinning field [Fig. 4(c1)].[16] The emergent DMI is responsible for specific remanent vortex-antivortex states [Fig. 4(a1)] in hollow toroidal nanomagnets[84] and curvature-induced selection of the winding number of a meron in hyperbolic [Fig. 4(a5)] and parabolic [Fig. 4(a6)] nanoshells.[78] A nonlocal chiral symmetry breaking leads to the selection of the handedness of the Néel domain wall in a complex 3D curved out-of-plane magnetized shell with a representative example of a generalized cylinder [Fig. 4(a2)].[64] Dynamical examples of chiral effects in flat wires include bounding of spin waves by a local bending of the wire due to the curvature-induced DMI,[111] the concept of a curvature-induced magnonic crystal by periodic deformation of the wire [Fig. 4(d1)].[94] Being driven by a gradient of the curvature of a nanostripe, transversal domain walls acquire remarkably high velocities free of the Walker limit.[112]

A spherical geometry is another testing area for chiral effects. In the case of easy-surface anisotropy, the emergent DMI is known[81] to be responsible for the polarity-chirality coupling, which means the

Published under an exclusive license by AIP Publishing

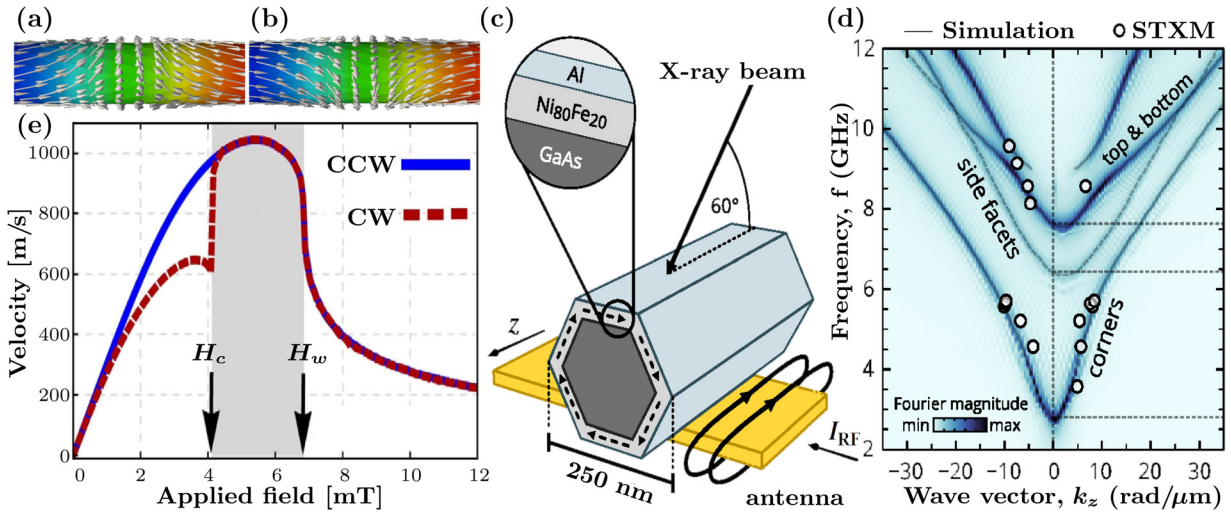

FIG. 3. Pattern-induced chirality breaking is stimulated by the chiral degenerated magnetic patterns with a nanotube as a paradigmatic example. (a), (b), and (e) Chiral breakdown of domain walls in a nanotube; (a) counterclockwise and (b) clockwise domain walls have different mobilities; (c) unfavorable clockwise wall changes its chirality during the motion: adapted from Ref. 85. (c) and (d) Experimental observation of the spitting of magnon spectrum in a hexagonal nanotube; (c) sketch of the hexagonal nanotube; and (e) dispersion of the spin waves: adapted from Ref. 76. (a), (b), and (e) are adapted from Otálora *et al.*, Appl. Phys. Lett. **100**, 072407 (2012). Copyright 2012 AIP Publishing LLC. (c) and (d) are adapted from Körber *et al.*, arXiv e-prints http://arxiv.org/abs/2009.02238; licensed under arXiv.org perpetual, non-exclusive license.

coupling between the well-localized perpendicular vortex core magnetization and the delocalized in-surface texture; the polarity-chirality coupling was also investigated for merons in parabolic and hyperbolic shells.[78] Spherical shells with perpendicular anisotropy support magnetic skyrmions even without intrinsic DMI[73,113] and can be simply induced by applying a uniform external magnetic field.[73] Magnetic skyrmions stabilized by the emergent DMI in a nanocap structure were observed by micromagnetic simulations.[114] Geometry-stabilized skyrmions are supported by various curved magnetic surfaces being driven by two different types of emergent DMI induced by the surface curvature: small-sized skyrmions are formed in the region of maximal curvature similar to the case of spherical shells;[73] tunable-size skyrmions are stabilized by the curvature gradient,[115] which refer to nanoindentations,[58,116] cone-shaped nanoshells,[117] and confined hole and trench materials.[118]

Geometrical manipulations of materials with intrinsic DMI give rise to mesoscale DMI [Fig. 4(b)] providing ample opportunities for geometrical manipulations of material responses.[74] One of them, a concept of artificial magnetoelectric materials [Fig. 4(b2)],[88] is elaborated for a specific example of torsional nanosprings, where the magnetic state is efficiently modified due to the change in geometrical parameters of the curved nanomagnet.[88] The interplay between two types of DMIs results in a new type of inclined domain walls [Fig. 4(b1)] in nanotubes.[87,119] For the spherical nanoshell, such an interplay favors skyrmions with different helicity numbers [Figs. 4(b3), 4(b5), and 4(b6)].[73] Namely, the interplay between two types of DMIs increases (decreases) the stability of skyrmions in dome (antidome) structures,[120] cylindrical nanostripes, and nanotubes.[121] A localized curvilinear defect can favor the multiplet of skyrmion states with a perspective to be utilized to encode and switch a bit of information.[89] Such a defect can pin a skyrmion, and the curvature-induced drift of the skyrmion is typically driven by the gradient of the local surface mean curvature [Fig. 4(c5)].[92] The periodically arranged lattice of the curvilinear defects can generate a skyrmion lattice [Fig. 4(b4)] as a ground state.[89]

Let us estimate typical lengthscales of geometry-governed interactions and compare them with the characteristic magnetic length ℓ and lengthscales of curvature-induced effects. Geometrically, the availability of the considered micromagnetic theory is limited by the relation $h \ll \mathscr{R}$, with h being the wire (film) thickness and $\mathscr{R}$ being the typical curvature radius.[70,71] Supposing that the typical size of magnetization inhomogeneity is about ℓ, one can estimate that geometry-governed emergent interactions driven by local emergent anisotropy and emergent DMI are well-pronounced for thin curved samples with $h < \ell$, while the nonlocal emergent interaction driven by magnetostatics appears for thicker samples with $h > \ell$.[64] In addition, curvature-induced effects become well pronounced when the curvature radii $\mathscr{R}$ decrease down to the magnetic length ℓ.[70,71]

We have discussed above a number of intriguing curvature-induced effects and their connection to emergent geometry-governed interactions. Most of these effects were only predicted theoretically and confirmed numerically. Therefore, it is important to outline the current state of the art of direct experimental observations of curvature-induced effects, which includes: experimentally quantified geometry-induced DMI in a flat parabolic stripe;[16] chiral anisotropic magnetoresistance of ferromagnetic microhelices;[122] a new angular dependence of magnetoelectrical response of a 3D nanomagnetic circuit;[123] observation of nonlocal chiral effects by asymmetric spin-wave dispersion in hexagonal nanotubes;[76] and experimentally observed influence of emergent DMI in Permalloy strips patterned into Archimedean spirals on the hysteresis loops with stepped behavior.[21]

IV. OUTLOOK AND FUTURE DIRECTIONS

By outlining the present state of the art of the curvilinear magnetism, here we focus on prospective directions that may prove to be of major importance to the field.

Published under an exclusive license by AIP Publishing

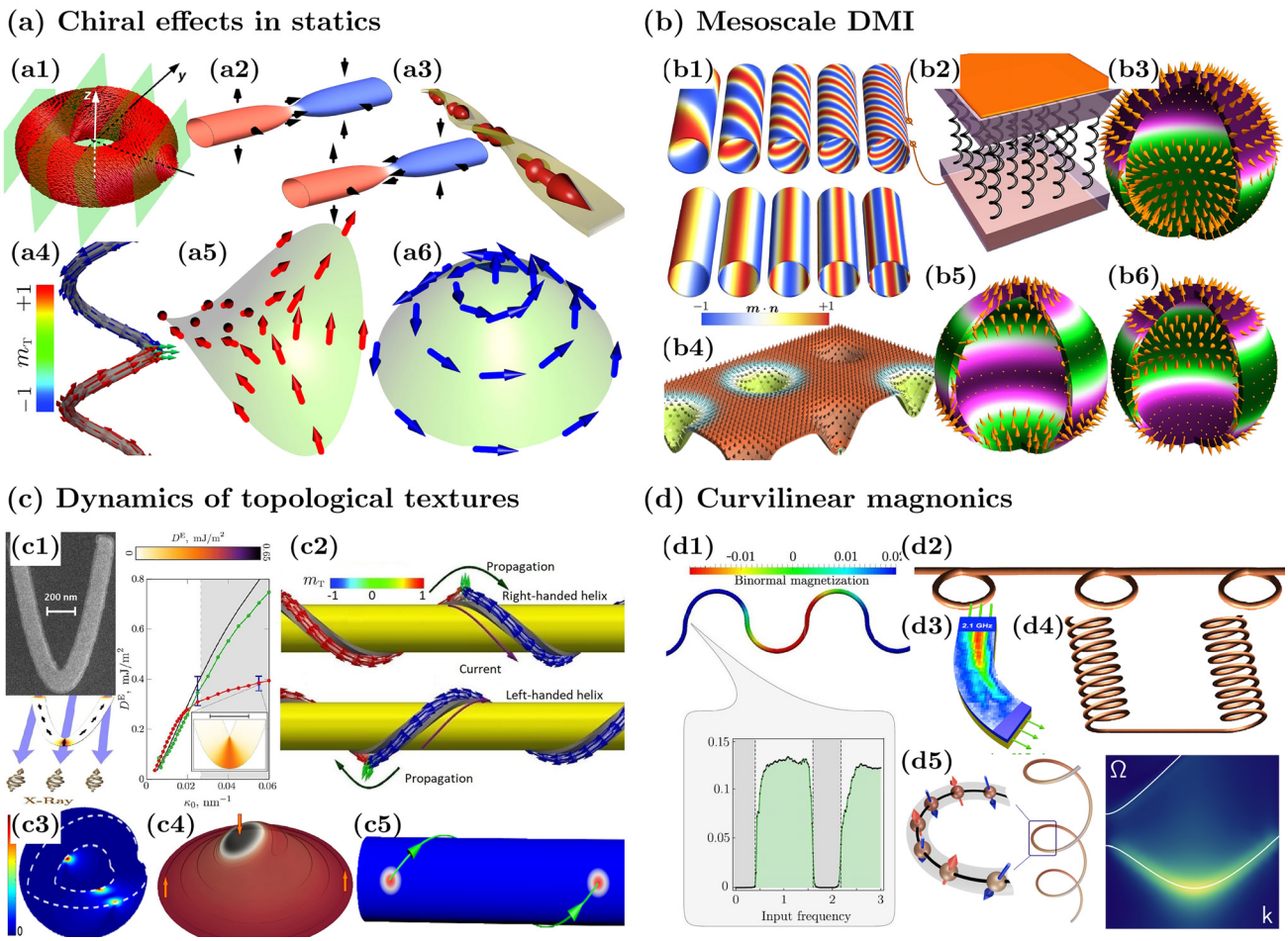

FIG. 4. Geometrically induced chirality breaking is a consequence of an interplay between the geometrical chirality of the object and the magnetochirality of the texture. Such chiral symmetry breaking results in a numerous static (a) and (b) and dynamic (c) and (d) effects. (a1) Formation of the vortex-antivortex pair in toroidal nanoshells: adapted from Vojkovic *et al.*, Appl. Phys. Lett. **121**, 113906 (2017).[84] Copyright 2017 AIP Publishing LLC. (a2) Selection of the domain wall handedness in a generalized cylinder: adapted with permission from Sheka *et al.*, Commun. Phys. **3**, 128 (2020).[64] Copyright 2020 Authors, licensed under a Creative Commons Attribution 4.0 International License. (a3) Selection of the handedness in a helicoid ribbon: adapted with permission from Gaididei *et al.*, J. Phys. A **50**, 385401 (2017).[86] Copyright 2017 IOP Publishing. (a4) Selection of the domain wall handedness in a helix wire: adapted with permission from Yershov *et al.*, Phys. Rev. B **93**, 094418 (2016).[79] Copyright 2016 American Physical Society. Selection of winding number of a meron in hyperbolic (a5) and parabolic (a6) nanoshells: reproduced with permission from Elías *et al.*, Sci. Rep. **9**, 14309 (2019).[78] Copyright 2019 Authors, licensed under a Creative Commons Attribution 4.0 International License. (b1) Inclined domain walls in nanotubes are realized due to the interplay between two types of DMI: adapted with permission from Yershov *et al.*, SciPost Phys. **9**, 43 (2020).[87] Copyright 2020 Authors, licensed under a Creative Commons Attribution 4.0 International License. (b2) Concept of artificial magnetoelectric materials: reproduced with permission from Volkov *et al.*, J. Phys. D: Appl. Phys. **52**, 345001 (2019).[88] Copyright 2019 IOP Publishing. (b4) Reconfigurable skyrmion lattice: reproduced with permission from Kravchuk *et al.*, Phys. Rev. Lett. **120**, 067201 (2018).[89] Copyright 2018 American Physical Society. (b3), (b5), and (b6) Skyrmions with different helicity numbers: reproduced with permission from Kravchuk *et al.*, Phys. Rev. B **94**, 144402 (2016).[73] Copyright 2016 American Physical Society. (c1) Quantified magnitude of emergent DMI in parabolic nanostripes: adapted with permission from Volkov *et al.*, Phys. Rev. Lett. **123**, 077201 (2019).[16] Copyright 2019 American Physical Society. (c2) The chirality sensitive domain wall mobility in helix wires: adapted with permission from Pylypovskyi *et al.*, Sci. Rep. **6**, 23316 (2016).[90] Copyright 2016 Authors, licensed under a Creative Commons Attribution 4.0 International License. (c3) Vortex dynamics in spherical shell: adapted with permission from McKeever *et al.*, Phys. Rev. B **100**, 054425 (2019).[91] Copyright 2019 American Physical Society. (c4) Skyrmion motion on a curved defect driven by the gradient of the surface curvature: reproduced with permission from Korniienko *et al.*, Phys. Rev. B **102**, 014432 (2020).[92] Copyright 2020 American Physical Society. (c5) Stable current-induced skyrmion propagation in a nanotube: reproduced with permission from Wang *et al.*, J. Phys. D: Appl. Phys. **52**, 225001 (2019).[93] Copyright 2019 IOP Publishing. (d1) Concept of curvature-induced magnonic crystal: adapted with permission from Korniienko *et al.*, SciPost Phys. **7**, 35 (2019).[94] Copyright 2019 Authors, licensed under a Creative Commons Attribution 4.0 International License. (d2) and (d4) Curved magnonic waveguides with designer bandgap spectrum: reproduced with permission from Tkachenko *et al.*, Appl. Phys. Lett. **101**, 152402 (2012).[95] Copyright 2012 AIP Publishing LLC. (d3) BLS detection of spin waves in curved micro-waveguide: reproduced with permission from Vogt *et al.*, Appl. Phys. Lett. **101**, 042410 (2012).[96] Copyright 2012 AIP Publishing LLC. (d5) Geometrically tunable spin-wave spectrum in the antiferromagnetic helix: reproduced with permission from Pylypovskyi *et al.*, Nano Lett. **20**, 8157–8162 (2020).[97] Copyright 2020 American Chemical Society.

Published under an exclusive license by AIP Publishing

A. Prospect for fundamental researches in curvilinear magnetism

Very recently, the generalized micromagnetic theory of curvilinear ferromagnets has been developed.[64] While this unified description allows discovering novel fundamental physical effects, there are still a number of open questions that are crucial for this research field.

1. Topologically protected magnetic states

Topologically protected magnetic states have found numerous applications, including information storage, magnetic random access memory, sensors, and neuromorphic computing devices. Curvilinear magnetism provides another route to realize topological textures by geometrical manipulations: namely, the topological patterning is responsible for the appearance of whirligig[66] and skyrmion[73] states in spherical shells, topologically induced domain walls in Möbius rings,[69] etc. The future challenge is to study *dynamics of topological magnetic solitons* [Fig. 4(c)] in curved magnets. This includes the problem of curvature-induced automotion of solitons: the first step in this direction was achieved recently by a concept of geometry-induced motion in the Euler spiral nanostripe.[112] Magnetic skyrmions are particle-like textures with prospective applications in racetrack-type devices,[124] where a curved track can guide the skyrmion motion.[125] By bending the films, one can pin the skyrmion by a geometrical defect[92] with the inertia term and a pinning potential are generated by the varying curvature:[126] the gradient of the curvature provides a driving force acting the skyrmions [Fig. 4(c4)].[92] We expect that automotion of solitons in curved magnetic wires and nanostripes will found applications in logic, ratchet, storage devices, where the topological defects can be passively moved in the part of device, in skyrmion Hall transport, where curved nanotrack will stabilize the skyrmion motion.

Another challenge is to describe current-driven transport problems of solitons in curved wires and curved films. Comprehensive studies of different domain walls dynamics in nanotubes already resulted in avoiding Walker breakdown[109] and appearance of chiral breakdown.[75,85,104,105] The domain wall dynamics in bent nanostripes is accompanied by the emergence of a second Walker-like critical field, corresponding to the reorientation of the domain wall phase.[127] Stable current-induced skyrmion propagation with a helical trajectory on magnetic nanotubes caused by the skyrmion Hall effect was predicted using micromagnetic simulations [Fig. 4(c5)].[93] A possibility to tune current-induced skyrmion motion by geometrical manipulations can overcome the skyrmion Hall effect, which is essential for skyrmionics applications. Particular interest is applied to the magnetic vortex dynamics in spherical particles. In particular, a field-induced linear vortex dynamics in spherical shells is studied in Ref. 91, and resonance modes are computed by micromagnetic simulations [Fig. 4(c3)]. Nutational dynamics of coupled vortices was studied numerically in Ref. 128. Resonantly excited precessional motion of a magnetic vortex core in soft magnetic spheres was studied analytically and numerically in Ref. 129. Controllable switching of chirality of a magnetic vortex[130] and chirality-dependent switching of the vortex core[131] in hemispherical caps structures have elucidated the role of curvature in switching phenomena. Further progress in curvilinear-geometry assisted switching phenomena and the current-driven dynamics of topologically protected states is important for potential applications in spintronics, skyrmionics, and spin logic.

2. Curvilinear antiferromagnetism

Curvilinear antiferromagnetism offers essential fundamental and application potentials. For basic studies, antiferromagnets serve several advantages in comparison with ferromagnets: (i) local types of interactions provided by the absence of stray fields, (ii) additional classes of topological defects, in particular antiferromagnetic disclinations, due to topological difference between the order parameters, and (iii) more complex, more reach, and in general more fast dynamics because of the presence of several exchange-enhanced sublattices. These aspects showcase antiferromagnets as key enablers of the prospective spintronic[132–134] and spin-orbitronic[135] technologies. To the moment, the general micromagnetic framework of curvilinear magnetism is constructed only for ferromagnets.[64] Geometrically curved antiferromagnets of a nontrivial topology support new topologically nontrivial states: in particular, the close loop geometry can favor kinklike solitons and Möbius states.[136] Very recently, a concept of curvilinear antiferromagnet was introduced for one-dimensional spin chains [Fig. 4(d5)].[97] An extension of theory beyond the σ-model allows to describe curvilinear 1D antiferomagnets and to determine conditions when they possess the geometry-driven weak ferromagnetism: in contrast to ferromagnets, antiferromagnets exhibit the geometry-driven modification of the magnetic responses stemming also from the anisotropy interaction.[137] Topological arguments about similarity between order parameters in attiferromagnets and liquid crystals[138] suggest that curvilinear antiferromagnets can support topological textures similar to liquid crystals, in particular, ground state disclinations,[139] and boojums.[140] The progress in the fundamental of curvilinear antiferromagnetism as well as development of applications could position curvilinear antiferromagnets as a novel platform for the realization of geometrically tunable chiral antiferromagnets for antiferromagnetic spintronics, spin-orbitronics, and magnonic devices relying on the geometrical curvature.

B. Prospect for applications of curved nanomagnets

1. Shapeable magnetoelectronics

Shapeable magnetoelectronics is a promising application direction where curvilinear magnetism is already applied. The concept of shapable magnetoelectronics[3] unites several families of magnetoelectronic devices, including stretchable,[141] flexible,[142] and printable[143] magnetosensitive elements. Shapable material technologies[3,4] allow to prepare complex 3D objects with applications to stretchable magnetic field sensorics,[5] energy storage devices,[26] and soft electronic skin.[144,145] Recently, a new approach to electric field controlled nanomagnets was proposed, which allows an electric field-induced deterministic switching between magnetic states without influencing intrinsic magnetic parameters.[88] Providing a possibility of tuning the magnetochiral properties of conventional magnetic materials using geometrical manipulations, this concept of *artificial magnetoelectric materials* should lead to a robust design of novel magnetoelectric devices.

2. Curvilinear magnonics

Curvilinear magnonics [Fig. 4(d)], being a part of rapidly developing 3D magnonics,[7] is an applied field, which actively uses tailored 3D nanoarchitectures. Curvilinear magnetic architectures enable to realize novel devices, such as ferromagnetic microtube ring resonators

Published under an exclusive license by AIP Publishing

fabricated by rolling up a layer system,[25] tunable spin-wave filters,[146] curved spin-wave lens[147] and family of on-chip rolled-up devices.[148] Recently, curvilinear magnetism has proposed several concepts, which seems to be prospective for 3D magnonics applications: a new type of magnonic crystals, curvature-induced ones, is proposed for ferromagnetic nanowires with periodically deformed shape [Fig. 4(d1)],[94] magnonic waveguides with designer bandgap spectrum [Figs. 4(d2) and 4(d4)],[95] filtering of magnon spectrum based on bounding of spin waves by local bending of a magnetic wire,[111] spin waves propagation over a distance ten times larger in the corrugated waveguide than that in the planar waveguides,[149] magnonic logic elements based on the nonreciprocity of the spin-wave spectrum in ferromagnet helix wires[77] and nanotubes,[102,103] 3D nanovolcanoes as multi-mode microwave resonators with potential applications in telecom-frequency filters,[46] and geometrically tunable magnon spectrum in an antiferromagnetic nanohelix [Fig. 4(d5)].[97]

3. Magnetic soft robotics

Magnetic soft robotics is another exciting area for applications of curvilinear magnetism. Recent break-neck growth of mobile microrobotics provides novel emergent classes of microrobot systems for various applications.[8,150] Soft robotics[151] deals with shapable materials. In particular, highly compliant and mechanically flexible magnets can perform different motion patterns when excited with an external magnetic field. They can be used to grip delicate objects very gently, transporting cargo, mimicking the movement of fast moving animals, and tissue engineering by mechanical stimulations.[152] To the moment, most of magnetically responsive flexible materials are magnetosensitive elastomers.[3–5,150] Their magnetic properties are determined by the nonlocal magnetostatic interaction, providing a relatively large scale of the geometrical deformations. Novel candidates for nanorobotics are organic and molecule-based magnets.[153] Magnetic properties of such elastic ferromagnets are essentially influenced by local interactions (exchange, anisotropy, and DMI), which enable size reduction of prospective devices in organic electronics and spintronics. The coupling between magnetic and mechanical subsystems in elastic ferromagnets can support spontaneous deformation of flexible enough planar film (or straight wire) induced by magnetic textures with such striking examples as soliton-induced deformation in cylindrical geometries[154,155] and skyrmion-induced deformation in planar films.[89] The shape transformation induced by the inhomogeneous magnetization texture was predicted for flexible ferromagnetic rings[156] and ribbons.[157] The deformation is effectively controlled by the external magnetic field with possible applications for soft nanorobotics[151] and soft magnetic sensorics.[5,158] Magnetic soft robotics, in particular, swimming microrobots, grant promising new tools for *in vivo* applications, such as diagnosis and therapy in complex environments, microsurgeries of individual cells, drug delivery, artificial fertilization techniques, etc.[159,160]

V. CONCLUDING REMARKS

Curvilinear magnetism is a field that, from the very beginning, has balanced between fundamental research, material sciences, and technologies.[1,2,6,10,11] Namely, advances and synergy between fundamentals and applications, their complementary expertise stimulates the development of new theoretical methods, novel fabrication, and characterization techniques as well as numerous applications. While fundamental proposals in curvilinear magnetism have been made only recently, we anticipate that this is an opportune time to explore the utility of 3D-shaped curved magnetic nanoarchitectures for electronics, spintronics, skyrmionics, magnonics, biomedicine, and soft robotics.

ACKNOWLEDGMENTS

I gratefully acknowledge valuable discussions with many past and present colleagues and also thank referees for their insightful remarks. This research was supported by the Alexander von Humboldt Foundation (Research Group Linkage Programme), by DFG via Grant No. MC 9/22–1, and by the Ministry of Education and Science of Ukraine (Project No. 19BF052–01).

DATA AVAILABILITY

Data sharing is not applicable to this article as no new data were created or analyzed in this study.

REFERENCES

[1]D. Sander, S. O. Valenzuela, D. Makarov, C. H. Marrows, E. E. Fullerton, P. Fischer, J. McCord, P. Vavassori, S. Mangin, P. Pirro, B. Hillebrands, A. D. Kent, T. Jungwirth, O. Gutfleisch, C. G. Kim, and A. Berger, "The 2017 magnetism roadmap," J. Phys. D: Appl. Phys. **50**, 363001 (2017).
[2]R. Streubel, P. Fischer, F. Kronast, V. P. Kravchuk, D. D. Sheka, Y. Gaididei, O. G. Schmidt, and D. Makarov, "Magnetism in curved geometries (topical review)," J. Phys. D: Appl. Phys. **49**, 363001 (2016).
[3]D. Makarov, M. Melzer, D. Karnaushenko, and O. G. Schmidt, "Shapeable magnetoelectronics," Appl. Phys. Rev. **3**, 011101 (2016).
[4]D. Karnaushenko, T. Kang, and O. G. Schmidt, "Shapeable material technologies for 3D self-assembly of mesoscale electronics," Adv. Mater. Technol. **4**, 1800692 (2019).
[5]M. Melzer, D. Makarov, and O. G. Schmidt, "A review on stretchable magnetic field sensorics," J. Phys. D: Appl. Phys. **53**, 083002 (2020).
[6]P. Fischer, D. Sanz-Hernández, R. Streubel, and A. Fernández-Pacheco, "Launching a new dimension with 3D magnetic nanostructures," APL Mater. **8**, 010701 (2020).
[7]*Three-Dimensional Magnonics: Layered, Micro- and Nanostructures*, 1st ed., edited by G. Gubbiotti (Jenny Stanford Publishing, 2019).
[8]M. Sitti, *Mobile Microrobotics* (MIT Press, Cambridge, MA, 2017).
[9]Y. Alapan, O. Yasa, B. Yigit, I. C. Yasa, P. Erkoc, and M. Sitti, "Microrobotics and microorganisms: Biohybrid autonomous cellular robots," Annu. Rev. Control, Rob., Auton. Syst. **2**, 205–230 (2019).
[10]E. Y. Vedmedenko, R. K. Kawakami, D. Sheka, P. Gambardella, A. Kirilyuk, A. Hirohata, C. Binek, O. A. Chubykalo-Fesenko, S. Sanvito, B. Kirby, J. Grollier, K. Everschor-Sitte, T. Kampfrath, C.-Y. You, and A. Berger, "The 2020 magnetism roadmap," J. Phys. D: Appl. Phys. **53**, 453001 (2020).
[11]A. Fernández-Pacheco, R. Streubel, O. Fruchart, R. Hertel, P. Fischer, and R. P. Cowburn, "Three-dimensional nanomagnetism," Nat. Commun. **8**, 15756 (2017).
[12]A. Westphalen, A. Remhof, and H. Zabel, "Magnetization reversal in nanowires with a spiral shape," J. Appl. Phys. **104**, 013906 (2008).
[13]G. Nahrwold, L. Bocklage, J. M. Scholtyssek, T. Matsuyama, B. Krüger, U. Merkt, and G. Meier, "Current-induced domain-wall depinning in curved permalloy nanowires," J. Appl. Phys. **105**, 07D511 (2009).
[14]E. R. Lewis, D. Petit, L. Thevenard, A. V. Jausovec, L. O'Brien, D. E. Read, and R. P. Cowburn, "Magnetic domain wall pinning by a curved conduit," Appl. Phys. Lett. **95**, 152505 (2009).
[15]J.-S. Kim, M.-A. Mawass, A. Bisig, B. Krüger, R. M. Reeve, T. Schulz, F. Büttner, J. Yoon, C.-Y. You, M. Weigand, H. Stoll, G. Schütz, H. J. M. Swagten, B. Koopmans, S. Eisebitt, and M. Kläui, "Synchronous precessional motion of multiple domain walls in a ferromagnetic nanowire by perpendicular field pulses," Nat. Commun. **5**, 3429 (2014).

Published under an exclusive license by AIP Publishing

[16]O. M. Volkov, A. Kákay, F. Kronast, I. Mönch, M.-A. Mawass, J. Fassbender, and D. Makarov, "Experimental observation of exchange-driven chiral effects in curvilinear magnetism," Phys. Rev. Lett. **123**, 077201 (2019).
[17]M. Kläui, C. A. F. Vaz, L. Lopez-Diaz, and J. A. C. Bland, "Vortex formation in narrow ferromagnetic rings," J. Phys.: Condens. Matter **15**, R985–R1024 (2003).
[18]F. J. Castano, C. A. Ross, C. Frandsen, A. Eilez, D. Gil, H. I. Smith, M. Redjdal, and F. B. Humphrey, "Metastable states in magnetic nanorings," Phys. Rev. B **67**, 184425 (2003).
[19]M.-A. Mawass, K. Richter, A. Bisig, R. M. Reeve, B. Krüger, M. Weigand, H. Stoll, A. Krone, F. Kronast, G. Schütz, and M. Kläui, "Switching by domain-wall automotion in asymmetric ferromagnetic rings," Phys. Rev. Appl. **7**, 044009 (2017).
[20]M. Nord, A. Semisalova, A. Kákay, G. Hlawacek, I. MacLaren, V. Liersch, O. M. Volkov, D. Makarov, G. W. Paterson, K. Potzger, J. Lindner, J. Fassbender, D. McGrouther, and R. Bali, "Strain anisotropy and magnetic domains in embedded nanomagnets," Small **15**, 1904738 (2019).
[21]V. Brajuskovic and C. Phatak, "Understanding curvature effects on the magnetization reversal of patterned permalloy archimedean spirals," Appl. Phys. Lett. **118**, 152409 (2021).
[22]J. G. Gibbs, A. G. Mark, T.-C. Lee, S. Eslami, D. Schamel, and P. Fischer, "Nanohelices by shadow growth," Nanoscale **6**, 9457 (2014).
[23]B. Dick, M. J. Brett, T. J. Smy, M. R. Freeman, M. Malac, and R. F. Egerton, "Periodic magnetic microstructures by glancing angle deposition," J. Vac. Sci. Technol. A **18**, 1838 (2000).
[24]E. J. Smith, D. Makarov, S. Sanchez, V. M. Fomin, and O. G. Schmidt, "Magnetic microhelix coil structures," Phys. Rev. Lett. **107**, 097204 (2011).
[25]F. Balhorn, S. Mansfeld, A. Krohn, J. Topp, W. Hansen, D. Heitmann, and S. Mendach, "Spin-wave interference in three-dimensional rolled-up ferromagnetic microtubes," Phys. Rev. Lett. **104**, 037205 (2010).
[26]F. Gabler, D. D. Karnaushenko, D. Karnaushenko, and O. G. Schmidt, "Magnetic origami creates high performance micro devices," Nat. Commun. **10**, 3013 (2019).
[27]T. Ozel, G. R. Bourret, and C. A. Mirkin, "Coaxial lithography," Nat. Nanotechnol. **10**, 319–324 (2015).
[28]R. Zierold, Z. Wu, J. Biskupek, U. Kaiser, J. Bachmann, C. E. Krill, and K. Nielsch, "Magnetic, multilayered nanotubes of low aspect ratios for liquid suspensions," Adv. Funct. Mater. **21**, 226–232 (2011).
[29]A. López-Ortega, M. Estrader, G. Salazar-Alvarez, A. G. Roca, and J. Nogués, "Applications of exchange coupled bi-magnetic hard/soft and soft/hard magnetic core/shell nanoparticles," Phys. Rep. **553**, 1–32 (2015).
[30]F. Sayed, N. Yaacoub, Y. Labaye, R. S. Hassan, G. Singh, P. A. Kumar, J. M. Greneche, R. Mathieu, G. C. Hadjipanayis, E. Agostinelli, and D. Peddis, "Surface effects in ultrathin iron oxide hollow nanoparticles: Exploring magnetic disorder at the nanoscale," J. Phys. Chem. C **122**, 7516–7524 (2018).
[31]S. Sahoo, S. Mondal, G. Williams, A. May, S. Ladak, and A. Barman, "Ultrafast magnetization dynamics in a nanoscale three-dimensional cobalt tetrapod structure," Nanoscale **10**, 9981–9986 (2018).
[32]G. Williams, M. Hunt, B. Boehm, A. May, M. Taverne, D. Ho, S. Giblin, D. Read, J. Rarity, R. Allenspach, and S. Ladak, "Two-photon lithography for 3D magnetic nanostructure fabrication," Nano Res. **11**, 845–854 (2018).
[33]J. Askey, M. O. Hunt, W. Langbein, and S. Ladak, "Use of two-photon lithography with a negative resist and processing to realise cylindrical magnetic nanowires," Nanomaterials **10**, 429 (2020).
[34]P. Pip, C. Donnelly, M. Döbeli, C. Gunderson, L. J. Heyderman, and L. Philippe, "Electroless deposition of Ni–Fe alloys on scaffolds for 3D nanomagnetism," Small **16**, 2004099 (2020).
[35]E. C. Burks, D. A. Gilbert, P. D. Murray, C. Flores, T. E. Felter, S. Charnvanichborikarn, S. O. Kucheyev, J. D. Colvin, G. Yin, and K. Liu, "3D nanomagnetism in low density interconnected nanowire networks," Nano Lett. **21**, 716–722 (2021).
[36]M. Huth, F. Porrati, and O. Dobrovolskiy, "Focused electron beam induced deposition meets materials science," Microelectron. Eng. **185–186**, 9–28 (2018).
[37]R. Winkler, J. D. Fowlkes, P. D. Rack, and H. Plank, "3D nanoprinting via focused electron beams," J. Appl. Phys. **125**, 210901 (2019).
[38]H. Plank, R. Winkler, C. H. Schwalb, J. Hütner, J. D. Fowlkes, P. D. Rack, I. Utke, and M. Huth, "Focused electron beam-based 3d nanoprinting for scanning probe microscopy: A review," Micromachines **11**, 48 (2019).
[39]A. Fernández-Pacheco, L. Skoric, J. M. D. Teresa, J. Pablo-Navarro, M. Huth, and O. V. Dobrovolskiy, "Writing 3D nanomagnets using focused electron beams," Materials **13**, 3774 (2020).
[40]A. Fernández-Pacheco, L. Serrano-Ramón, J. M. Michalik, M. R. Ibarra, J. M. D. Teresa, L. O'Brien, D. Petit, J. Lee, and R. P. Cowburn, "Three dimensional magnetic nanowires grown by focused electron-beam induced deposition," Sci. Rep. **3**, 1492 (2013).
[41]Y. M. Lau, P. C. Chee, J. T. L. Thong, and V. Ng, "Properties and applications of cobalt-based material produced by electron-beam-induced deposition," J. Vac. Sci. Technol. A **20**, 1295–1302 (2002).
[42]C. Phatak, C. S. Miller, Z. Thompson, E. B. Gulsoy, and A. K. Petford-Long, "Curved three-dimensional cobalt nanohelices for use in domain wall device applications," ACS Appl. Nano Mater. **3**, 6009 (2020).
[43]D. Sanz-Hernández, A. Hierro-Rodriguez, C. Donnelly, J. Pablo-Navarro, A. Sorrentino, E. Pereiro, C. Magén, S. McVitie, J. M. de Teresa, S. Ferrer, P. Fischer, and A. Fernández-Pacheco, "Artificial double-helix for geometrical control of magnetic chirality," ACS Nano **14**, 8084 (2020).
[44]L. Keller, M. K. I. A. Mamoori, J. Pieper, C. Gspan, I. Stockem, C. Schröder, S. Barth, R. Winkler, H. Plank, M. Pohlit, J. Müller, and M. Huth, "Direct-write of free-form building blocks for artificial magnetic 3D lattices," Sci. Rep. **8**, 6160 (2018).
[45]L. Skoric, D. Sanz-Hernández, F. Meng, C. Donnelly, S. Merino-Aceituno, and A. Fernández-Pacheco, "Layer-by-layer growth of complex-shaped three-dimensional nanostructures with focused electron beams," Nano Lett. **20**, 184–191 (2020).
[46]O. V. Dobrovolskiy, N. R. Vovk, A. V. Bondarenko, S. A. Bunyaev, S. Lamb-Camarena, N. Zenbaa, R. Sachser, S. Barth, K. Y. Guslienko, A. V. Chumak, M. Huth, and G. N. Kakazei, "Spin-wave eigenmodes in direct-write 3D nanovolcanoes," Appl. Phys. Lett. **118**, 132405 (2021).
[47]C. Phatak, Y. Liu, E. B. Gulsoy, D. Schmidt, E. Franke-Schubert, and A. Petford-Long, "Visualization of the magnetic structure of sculpted three-dimensional Cobalt nanospirals," Nano Lett. **14**, 759–764 (2014).
[48]D. Sanz-Hernández, R. F. Hamans, J.-W. Liao, A. Welbourne, R. Lavrijsen, and A. Fernández-Pacheco, "Fabrication, detection, and operation of a three-dimensional nanomagnetic conduit," ACS Nano **11**, 11066–11073 (2017).
[49]S. O. Demokritov, B. Hillebrands, and A. N. Slavin, "Brillouin light scattering studies of confined spin waves: Linear and nonlinear confinement," Phys. Rep. **348**, 441–489 (2001).
[50]C. Gatel, F. J. Bonilla, A. Meffre, E. Snoeck, B. Warot-Fonrose, B. Chaudret, L.-M. Lacroix, and T. Blon, "Size-specific spin configurations in single iron nanomagnet: From flower to exotic vortices," Nano Lett. **15**, 6952–6957 (2015).
[51]I. Gross, W. Akhtar, V. Garcia, L. J. Martínez, S. Chouaieb, K. Garcia, C. Carrétéro, A. Barthélémy, P. Appel, P. Maletinsky, J.-V. Kim, J. Y. Chauleau, N. Jaouen, M. Viret, M. Bibes, S. Fusil, and V. Jacques, "Real-space imaging of non-collinear antiferromagnetic order with a single-spin magnetometer," Nature **549**, 252–256 (2017).
[52]N. Hedrich, K. Wagner, O. V. Pylypovskyi, B. J. Shields, T. Kosub, D. D. Sheka, D. Makarov, and P. Maletinsky, "Nanoscale mechanics of antiferromagnetic domain walls," Nat. Phys. **17**, 574 (2021).
[53]C. Phatak, M. Beleggia, and M. De Graef, "Vector field electron tomography of magnetic materials: Theoretical development," Ultramicroscopy **108**, 503–513 (2008).
[54]C. Phatak and D. Gürsoy, "Iterative reconstruction of magnetic induction using lorentz transmission electron tomography," Ultramicroscopy **150**, 54–64 (2015).
[55]C. Donnelly, M. Guizar-Sicairos, V. Scagnoli, S. Gliga, M. Holler, J. Raabe, and L. J. Heyderman, "Three-dimensional magnetization structures revealed with x-ray vector nanotomography," Nature **547**, 328–331 (2017).
[56]R. Streubel, F. Kronast, P. Fischer, D. Parkinson, O. G. Schmidt, and D. Makarov, "Retrieving spin textures on curved magnetic thin films with full-field soft X-ray microscopies," Nat. Commun. **6**, 7612 (2015).
[57]K. Witte, A. Späth, S. Finizio, C. Donnelly, B. Watts, B. Sarafimov, M. Odstrcil, M. Guizar-Sicairos, M. Holler, R. H. Fink, and J. Raabe, "From 2D STXM to 3D imaging: Soft X-ray laminography of thin specimens," Nano Lett. **20**, 1305–1314 (2020).

Published under an exclusive license by AIP Publishing

[58]D. Makarov, L. Baraban, I. L. Guhr, J. Boneberg, H. Schift, J. Gobrecht, G. Schatz, P. Leiderer, and M. Albrecht, "Arrays of magnetic nanoindentations with perpendicular anisotropy," Appl. Phys. Lett. **90**, 093117 (2007).
[59]D. K. Ball, K. Lenz, M. Fritzsche, G. Varvaro, S. Günther, P. Krone, D. Makarov, A. Mücklich, S. Facsko, J. Faßbender, and M. Albrecht, "Magnetic properties of granular CoCrPt:SiO 2 thin films deposited on GaSb nanocones," Nanotechnology **25**, 085703 (2014).
[60]V. V. Slastikov and C. Sonnenberg, "Reduced models for ferromagnetic nanowires," IMA J. Appl. Math. **77**, 220–235 (2012).
[61]V. Slastikov, "Micromagnetism of thin shells," Math. Models Methods Appl. Sci. **15**, 1469–1487 (2005).
[62]G. D. Fratta, C. B. Muratov, F. N. Rybakov, and V. V. Slastikov, "Variational principles of micromagnetics revisited," SIAM J. Math. Anal. **52**, 3580–3599 (2020).
[63]G. D. Fratta, "Micromagnetics of curved thin films," Z. Angew. Math. Phys. **71**, 111 (2020).
[64]D. D. Sheka, O. V. Pylypovskyi, P. Landeros, Y. Gaididei, A. Kákay, and D. Makarov, "Nonlocal chiral symmetry breaking in curvilinear magnetic shells," Commun. Phys. **3**, 128 (2020).
[65]J. A. López-López, D. Cortés-Ortuño, and P. Landeros, "Role of anisotropy on the domain wall properties of ferromagnetic nanotubes," J. Magn. Magn. Mater. **324**, 2024–2029 (2012).
[66]M. I. Sloika, D. D. Sheka, V. P. Kravchuk, O. V. Pylypovskyi, and Y. Gaididei, "Geometry induced phase transitions in magnetic spherical shell," J. Magn. Magn. Mater. **443**, 404–412 (2017).
[67]A. Teixeira, S. Castillo-Sepúlveda, S. Vojkovic, J. Fonseca, D. Altbir, Á. Núñez, and V. Carvalho-Santos, "Analysis on the stability of in-surface magnetic configurations in toroidal nanoshells," J. Magn. Magn. Mater. **478**, 253–259 (2019).
[68]V. Carvalho-Santos, R. Elias, D. Altbir, and J. Fonseca, "Stability of skyrmions on curved surfaces in the presence of a magnetic field," J. Magn. Magn. Mater. **391**, 179–183 (2015).
[69]O. V. Pylypovskyi, V. P. Kravchuk, D. D. Sheka, D. Makarov, O. G. Schmidt, and Y. Gaididei, "Coupling of chiralities in spin and physical spaces: The Möbius ring as a case study," Phys. Rev. Lett. **114**, 197204 (2015).
[70]Y. Gaididei, V. P. Kravchuk, and D. D. Sheka, "Curvature effects in thin magnetic shells," Phys. Rev. Lett. **112**, 257203 (2014).
[71]D. D. Sheka, V. P. Kravchuk, and Y. Gaididei, "Curvature effects in statics and dynamics of low dimensional magnets," J. Phys. A **48**, 125202 (2015).
[72]B. Göbel, I. Mertig, and O. A. Tretiakov, "Beyond skyrmions: Review and perspectives of alternative magnetic quasiparticles," Phys. Rep. **895**, 1–28 (2021).
[73]V. P. Kravchuk, U. K. Rößler, O. M. Volkov, D. D. Sheka, J. van den Brink, D. Makarov, H. Fuchs, H. Fangohr, and Y. Gaididei, "Topologically stable magnetization states on a spherical shell: Curvature-stabilized skyrmions," Phys. Rev. B **94**, 144402 (2016).
[74]O. M. Volkov, D. D. Sheka, Y. Gaididei, V. P. Kravchuk, U. K. Rößler, J. Fassbender, and D. Makarov, "Mesoscale Dzyaloshinskii-Moriya interaction: Geometrical tailoring of the magnetochirality," Sci. Rep. **8**, 866 (2018).
[75]P. Landeros and A. S. Núñez, "Domain wall motion on magnetic nanotubes," J. Appl. Phys. **108**, 033917 (2010).
[76]L. Körber, M. Zimmermann, S. Wintz, S. Finizio, M. Weigand, J. Raabe, J. A. Otálora, H. Schultheiss, E. Josten, J. Lindner, C. H. Back, and A. Kákay, "Experimental observation of the curvature-induced asymmetric spin-wave dispersion in hexagonal nanotubes," e-prints arXiv:2009.02238 (2020).
[77]D. D. Sheka, V. P. Kravchuk, K. V. Yershov, and Y. Gaididei, "Torsion-induced effects in magnetic nanowires," Phys. Rev. B **92**, 054417 (2015).
[78]R. G. Elías, N. Vidal-Silva, and V. L. Carvalho-Santos, "Winding number selection on merons by Gaussian curvature's sign," Sci. Rep. **9**, 14309 (2019).
[79]K. V. Yershov, V. P. Kravchuk, D. D. Sheka, and Y. Gaididei, "Curvature and torsion effects in spin-current driven domain wall motion," Phys. Rev. B **93**, 094418 (2016).
[80]A. González, P. Landeros, and Á. S. Núñez, "Spin wave spectrum of magnetic nanotubes," J. Magn. Magn. Mater. **322**, 530–535 (2010).
[81]V. P. Kravchuk, D. D. Sheka, R. Streubel, D. Makarov, O. G. Schmidt, and Y. Gaididei, "Out-of-surface vortices in spherical shells," Phys. Rev. B **85**, 144433 (2012).
[82]M. Staňo and O. Fruchart, "Magnetic nanowires and nanotubes," in *Handbook of Magnetic Materials* (Elsevier, 2018), pp. 155–267.
[83]S. Da Col, S. Jamet, N. Rougemaille, A. Locatelli, T. O. Mentes, B. S. Burgos, R. Afid, M. Darques, L. Cagnon, J. C. Toussaint, and O. Fruchart, "Observation of Bloch-point domain walls in cylindrical magnetic nanowires," Phys. Rev. B **89**(R), 180405 (2014).
[84]S. Vojkovic, V. L. Carvalho-Santos, J. M. Fonseca, and A. S. Nunez, "Vortex-antivortex pairs induced by curvature in toroidal nanomagnets," J. Appl. Phys. **121**, 113906 (2017).
[85]J. Otálora, J. López-López, P. Vargas, and P. Landeros, "Chirality switching and propagation control of a vortex domain wall in ferromagnetic nanotubes," Appl. Phys. Lett. **100**, 072407 (2012).
[86]Y. Gaididei, A. Goussev, V. P. Kravchuk, O. V. Pylypovskyi, J. M. Robbins, D. Sheka, V. Slastikov, and S. Vasylkevych, "Magnetization in narrow ribbons: Curvature effects," J. Phys. A **50**, 385401 (2017).
[87]K. Yershov, V. Kravchuk, D. Sheka, and U. Roessler, "Curvature effects on phase transitions in chiral magnets," SciPost Phys. **9**, 43 (2020).
[88]O. Volkov, U. K. Rößler, J. Fassbender, and D. Makarov, "Concept of artificial magnetoelectric materials via geometrically controlling curvilinear helimagnets," J. Phys. D: Appl. Phys. **52**, 345001 (2019).
[89]V. P. Kravchuk, D. D. Sheka, A. Kákay, O. M. Volkov, U. K. Rößler, J. van den Brink, D. Makarov, and Y. Gaididei, "Multiplet of skyrmion states on a curvilinear defect: Reconfigurable skyrmion lattices," Phys. Rev. Lett. **120**, 067201 (2018).
[90]O. V. Pylypovskyi, D. D. Sheka, V. P. Kravchuk, K. V. Yershov, D. Makarov, and Y. Gaididei, "Rashba torque driven domain wall motion in magnetic helices," Sci. Rep. **6**, 23316 (2016).
[91]C. McKeever, F. Y. Ogrin, and M. M. Aziz, "Microwave magnetization dynamics in ferromagnetic spherical nanoshells," Phys. Rev. B **100**, 054425 (2019).
[92]A. Korniienko, A. Kákay, D. D. Sheka, and V. P. Kravchuk, "Effect of curvature on the eigenstates of magnetic skyrmions," Phys. Rev. B **102**, 014432 (2020).
[93]X. Wang, X. S. Wang, C. Wang, H. Yang, Y. Cao, and P. Yan, "Current-induced skyrmion motion on magnetic nanotubes," J. Phys. D: Appl. Phys. **52**, 225001 (2019).
[94]A. Korniienko, V. Kravchuk, O. Pylypovskyi, D. Sheka, J. van den Brink, and Y. Gaididei, "Curvature induced magnonic crystal in nanowires," SciPost Phys. **7**, 35 (2019).
[95]V. S. Tkachenko, A. N. Kuchko, M. Dvornik, and V. V. Kruglyak, "Propagation and scattering of spin waves in curved magnonic waveguides," Appl. Phys. Lett. **101**, 152402 (2012).
[96]K. Vogt, H. Schultheiss, S. Jain, J. E. Pearson, A. Hoffmann, S. D. Bader, and B. Hillebrands, "Spin waves turning a corner," Appl. Phys. Lett. **101**, 042410 (2012).
[97]O. V. Pylypovskyi, D. Y. Kononenko, K. V. Yershov, U. K. Rößler, A. V. Tomilo, J. Fassbender, J. van den Brink, D. Makarov, and D. D. Sheka, "Curvilinear one-dimensional antiferromagnets," Nano Lett. **20**, 8157–8162 (2020).
[98]G. Chen and A. K. Schmid, "Imaging and tailoring the chirality of domain walls in magnetic films," Adv. Mater. **27**, 5738–5743 (2015).
[99]A. Hubert and R. Schäfer, *Magnetic Domains: The Analysis of Magnetic Microstructures* (Springer Berlin Heidelberg, Berlin, 2009).
[100]*Topological Structures in Ferroic Materials*, edited by J. Seidel (Springer International Publishing, Switzerland, 2016).
[101]M. Zimmermann, T. N. G. Meier, F. Dirnberger, A. Kákay, M. Decker, S. Wintz, S. Finizio, E. Josten, J. Raabe, M. Kronseder, D. Bougeard, J. Lindner, and C. H. Back, "Origin and manipulation of stable vortex ground states in permalloy nanotubes," Nano Lett. **18**, 2828–2834 (2018).
[102]J. A. Otálora, M. Yan, H. Schultheiss, R. Hertel, and A. Kákay, "Curvature-induced asymmetric spin-wave dispersion," Phys. Rev. Lett. **117**, 227203 (2016).
[103]J. A. Otálora, M. Yan, H. Schultheiss, R. Hertel, and A. Kákay, "Asymmetric spin-wave dispersion in ferromagnetic nanotubes induced by surface curvature," Phys. Rev. B **95**, 184415 (2017).
[104]M. Yan, C. Andreas, A. Kákay, F. Garcia-Sanchez, and R. Hertel, "Chiral symmetry breaking and pair-creation mediated Walker breakdown in magnetic nanotubes," Appl. Phys. Lett. **100**, 252401 (2012).

Published under an exclusive license by AIP Publishing

[105]J. Otálora, J. López-López, P. Landeros, P. Vargas, and A. S. Núñez, "Breaking of chiral symmetry in vortex domain wall propagation in ferromagnetic nanotubes," J. Magn. Magn. Mater. **341**, 86–92 (2013).
[106]R. Hertel, "Curvature–induced magnetochirality," SPIN **03**, 1340009 (2013).
[107]M. Yan, C. Andreas, A. Kákay, F. García-Sánchez, and R. Hertel, "Fast domain wall dynamics in magnetic nanotubes: Suppression of Walker breakdown and Cherenkov-like spin wave emission," Appl. Phys. Lett. **99**, 122505 (2011).
[108]M. Yan, A. Kákay, C. Andreas, and R. Hertel, "Spin-Cherenkov effect and magnonic Mach cones," Phys. Rev. B **88**, 220412 (2013).
[109]M. Yan, A. Kákay, S. Gliga, and R. Hertel, "Beating the Walker limit with massless domain walls in cylindrical nanowires," Phys. Rev. Lett. **104**, 057201 (2010).
[110]K. V. Yershov, V. P. Kravchuk, D. D. Sheka, and Y. Gaididei, "Curvature-induced domain wall pinning," Phys. Rev. B **92**, 104412 (2015).
[111]Y. Gaididei, V. P. Kravchuk, F. G. Mertens, O. V. Pylypovskyi, A. Saxena, D. D. Sheka, and O. M. Volkov, "Localization of magnon modes in a curved magnetic nanowire," Low Temp. Phys. **44**, 634–643 (2018).
[112]K. V. Yershov, V. P. Kravchuk, D. D. Sheka, O. V. Pylypovskyi, D. Makarov, and Y. Gaididei, "Geometry-induced motion of magnetic domain walls in curved nanostripes," Phys. Rev. B **98**(R), 060409 (2018).
[113]C. Melcher and Z. N. Sakellaris, "Curvature-stabilized skyrmions with angular momentum," Lett. Math. Phys. **109**, 2291 (2019).
[114]J. Yang, C. Abert, D. Suess, and S.-K. Kim, "Intrinsic DMI-free skyrmion formation and robust dynamic behaviors in magnetic hemispherical shells," Sci. Rep. **11**, 3886 (2021).
[115]O. V. Pylypovskyi, D. Makarov, V. P. Kravchuk, Y. Gaididei, A. Saxena, and D. D. Sheka, "Chiral skyrmion and skyrmionium states engineered by the gradient of curvature," Phys. Rev. Appl. **10**, 064057 (2018).
[116]C. Schulze, M. Faustini, J. Lee, H. Schletter, M. U. Lutz, P. Krone, M. Gass, K. Sader, A. L. Bleloch, M. Hietschold, M. Fuger, D. Suess, J. Fidler, U. Wolff, V. Neu, D. Grosso, D. Makarov, and M. Albrecht, "Magnetic films on nanoperforated templates: A route towards percolated perpendicular media," Nanotechnology **21**, 495701 (2010).
[117]D. K. Ball, S. Günther, M. Fritzsche, K. Lenz, G. Varvaro, S. Laureti, D. Makarov, A. Mücklich, S. Facsko, M. Albrecht, and J. Fassbender, "Out-of-plane magnetized cone-shaped magnetic nanoshells," J. Phys. D: Appl. Phys. **50**, 115004 (2017).
[118]G. Qin, Y. Wang, K. Pei, R. Zhang, C. Zhang, Y. Luo, J. Cao, and R. Che, "Skyrmion bubbles stabilization in confined hole and trench materials," Appl. Phys. Lett. **117**, 052405 (2020).
[119]Y. Liu, N. Cai, X. Yu, and S. Xuan, "Nucleation and stability of skyrmions in three-dimensional chiral nanostructures," Sci. Rep. **10**, 21717 (2020).
[120]V. L. Carvalho-Santos, R. M. Corona, D. Altbir, and S. Castillo-Sepúlveda, "Shifts in the skyrmion stabilization due to curvature effects in dome- and antidome-shaped surfaces," Phys. Rev. B **102**, 024444 (2020).
[121]D. Kechrakos, L. Tzannetou, and A. Patsopoulos, "Magnetic skyrmions in cylindrical ferromagnetic nanostructures with chiral interactions," Phys. Rev. B **102**, 054439 (2020).
[122]H. Maurenbrecher, J. Mendil, G. Chatzipirpiridis, M. Mattmann, S. Pané, B. J. Nelson, and P. Gambardella, "Chiral anisotropic magnetoresistance of ferromagnetic helices," Appl. Phys. Lett. **112**, 242401 (2018).
[123]F. Meng, C. Donnelly, C. Abert, L. Skoric, S. Holmes, Z. Xiao, J.-W. Liao, P. J. Newton, C. H. Barnes, D. Sanz-Hernández, A. Hierro-Rodriguez, D. Suess, R. P. Cowburn, and A. Fernández-Pacheco, "Non-planar geometrical effects on the magnetoelectrical signal in a three-dimensional nanomagnetic circuit," ACS Nano **15**, 6765 (2021).
[124]C. Back, V. Cros, H. Ebert, K. Everschor-Sitte, A. Fert, M. Garst, T. Ma, S. Mankovsky, T. L. Monchesky, M. Mostovoy, N. Nagaosa, S. S. P. Parkin, C. Pfleiderer, N. Reyren, A. Rosch, Y. Taguchi, Y. Tokura, K. von Bergmann, and J. Zang, "The 2020 skyrmionics roadmap," J. Phys. D: Appl. Phys. **53**, 363001 (2020).
[125]I. Purnama, W. L. Gan, D. W. Wong, and W. S. Lew, "Guided current-induced skyrmion motion in 1d potential well," Sci. Rep. **5**, 10620 (2015).
[126]A. Pavlis and C. Psaroudaki, "Curvature-induced skyrmion mass," Phys. Rev. Res. **2**, 032058 (2020).
[127]G. H. R. Bittencourt, R. Moreno, R. Cacilhas, S. Castillo-Sepúlveda, O. Chubykalo-Fesenko, D. Altbir, and V. L. Carvalho-Santos, "Curvature-induced emergence of a second critical field for domain wall dynamics in bent nanostripes," Appl. Phys. Lett. **118**, 142405 (2021).
[128]J.-H. Lee, J. Kim, M.-K. Kim, J. Sim, and S.-K. Kim, "Nutation-like-mode excitation of coupled vortex cores in magnetic spherical shells," J. Appl. Phys. **122**, 233903 (2017).
[129]S.-K. Kim, M.-W. Yoo, J. Lee, H.-Y. Lee, J.-H. Lee, Y. Gaididei, V. P. Kravchuk, and D. D. Sheka, "Resonantly excited precession motion of three-dimensional vortex core in magnetic nanospheres," Sci. Rep. **5**, 11370 (2015).
[130]K. V. Yershov, V. P. Kravchuk, D. D. Sheka, and Y. Gaididei, "Controllable vortex chirality switching on spherical shells," J. Appl. Phys. **117**, 083908 (2015).
[131]M. I. Sloika, V. P. Kravchuk, D. D. Sheka, and Y. Gaididei, "Curvature induced chirality symmetry breaking in vortex core switching phenomena," Appl. Phys. Lett. **104**, 252403 (2014).
[132]O. Gomonay, T. Jungwirth, and J. Sinova, "Concepts antiferromagnetic spintronics," Phys. Status Solidi RRL **11**, 1700022 (2017).
[133]V. Baltz, A. Manchon, M. Tsoi, T. Moriyama, T. Ono, and Y. Tserkovnyak, "Antiferromagnetic spintronics," Rev. Mod. Phys. **90**, 015005 (2018).
[134]L. Šmejkal, Y. Mokrousov, B. Yan, and A. H. MacDonald, "Topological antiferromagnetic spintronics," Nat. Phys. **14**, 242–251 (2018).
[135]A. Manchon, J. Železný, I. M. Miron, T. Jungwirth, J. Sinova, A. Thiaville, K. Garello, and P. Gambardella, "Current-induced spin-orbit torques in ferromagnetic and antiferromagnetic systems," Rev. Mod. Phys. **91**, 035004 (2019).
[136]S. Castillo-Sepúlveda, R. A. Escobar, D. Altbir, M. Krizanac, and E. Y. Vedmedenko, "Magnetic Möbius stripe without frustration: Noncollinear metastable states," Phys. Rev. B **96**, 024426 (2017).
[137]O. V. Pylypovskyi, Y. A. Borysenko, J. Fassbender, D. D. Sheka, and D. Makarov, "Curvature-driven homogeneous Dzyaloshinskii-Moriya interaction and emergent weak ferromagnetism in anisotropic antiferromagnetic spin chains," Appl. Phys. Lett. **118**, 182405 (2021).
[138]G. Napoli, O. V. Pylypovskyi, D. D. Sheka, and L. Vergori, "Nematic versus ferromagnetic shells: New insights in curvature-induced effects," e-prints arXiv:2102.13497 (2021).
[139]V. Vitelli and D. R. Nelson, "Nematic textures in spherical shells," Phys. Rev. E **74**, 021711 (2006).
[140]M. Kleman and O. D. Lavrentovich, "Topological point defects in nematic liquid crystals," Philos. Mag. **86**, 4117–4137 (2006).
[141]M. Melzer, D. Makarov, A. Calvimontes, D. Karnaushenko, S. Baunack, R. Kaltofen, Y. Mei, and O. G. Schmidt, "Stretchable magnetoelectronics," Nano Lett. **11**, 2522–2526 (2011).
[142]M. Melzer, J. I. Mönch, D. Makarov, Y. Zabila, G. S. Cañón Bermúdez, D. Karnaushenko, S. Baunack, F. Bahr, C. Yan, M. Kaltenbrunner, and O. G. Schmidt, "Wearable magnetic field sensors for flexible electronics," Adv. Mater. **27**, 1274–1280 (2015).
[143]D. Makarov, D. Karnaushenko, and O. G. Schmidt, "Printable magnetoelectronics," ChemPhysChem **14**, 1771–1776 (2013).
[144]G. S. C. Bermúdez, D. D. Karnaushenko, D. Karnaushenko, A. Lebanov, L. Bischoff, M. Kaltenbrunner, J. Fassbender, O. G. Schmidt, and D. Makarov, "Magnetosensitive e-skins with directional perception for augmented reality," Sci. Adv. **4**, eaao2623 (2018).
[145]J. Ge, X. Wang, M. Drack, O. Volkov, M. Liang, G. S. C. Bermúdez, R. Illing, C. Wang, S. Zhou, J. Fassbender, M. Kaltenbrunner, and D. Makarov, "A bimodal soft electronic skin for tactile and touchless interaction in real time," Nat. Commun. **10**, 4405 (2019).
[146]F. Balhorn, S. Jeni, W. Hansen, D. Heitmann, and S. Mendach, "Axial and azimuthal spin-wave eigenmodes in rolled-up permalloy stripes," Appl. Phys. Lett. **100**, 222402 (2012).
[147]J.-N. Toedt, M. Mundkowski, D. Heitmann, S. Mendach, and W. Hansen, "Design and construction of a spin-wave lens," Sci. Rep. **6**, 33169 (2016).
[148]E. J. Smith, W. Xi, D. Makarov, I. Mönch, S. Harazim, V. A. B. Quiñones, C. K. Schmidt, Y. Mei, S. Sanchez, and O. G. Schmidt, "Lab-in-a-tube: Ultracompact components for on-chip capture and detection of individual micro-/nanoorganisms," Lab Chip **12**, 1917 (2012).
[149]I. Turčan, L. Flajšman, O. Wojewoda, V. Roučka, O. Man, and M. Urbánek, "Spin wave propagation in corrugated waveguides," Appl. Phys. Lett. **118**, 092405 (2021).
[150]M. Sitti and D. S. Wiersma, "Pros and cons: Magnetic versus optical microrobots," Adv. Mater. **32**, 1906766 (2020).

Published under an exclusive license by AIP Publishing

[151]D. Rus and M. T. Tolley, "Design, fabrication and control of soft robots," Nature **521**, 467–475 (2015).
[152]W. Hu, G. Z. Lum, M. Mastrangeli, and M. Sitti, "Small-scale soft-bodied robot with multimodal locomotion," Nat. **554**, 81–85 (2018).
[153]J. S. Miller, "Organic- and molecule-based magnets," Mater. Today **17**, 224–235 (2014).
[154]R. Dandoloff, S. Villain-Guillot, A. Saxena, and A. R. Bishop, "Violation of self-duality for topological solitons due to soliton-soliton interaction on a cylindrical geometry," Phys. Rev. Lett. **74**, 813–815 (1995).
[155]A. Saxena, R. Dandoloff, and T. Lookman, "Deformable curved magnetic surfaces," Physica A **261**, 13–25 (1998).
[156]Y. Gaididei, K. V. Yershov, D. D. Sheka, V. P. Kravchuk, and A. Saxena, "Magnetization-induced shape transformations in flexible ferromagnetic rings," Phys. Rev. B **99**, 014404 (2019).
[157]K. V. Yershov, V. P. Kravchuk, D. D. Sheka, J. van den Brink, and Y. Gaididei, "Spontaneous deformation of flexible ferromagnetic ribbons induced by Dzyaloshinskii-Moriya interaction," Phys. Rev. B **100**(R), 140407 (2019).
[158]J. Wang, M.-F. Lin, S. Park, and P. S. Lee, "Deformable conductors for human–machine interface," Mater. Today **21**, 508–526 (2018).
[159]M. Medina-Sánchez, V. Magdanz, M. Guix, V. M. Fomin, and O. G. Schmidt, "Swimming microrobots: Soft, reconfigurable, and smart," Adv. Funct. Mater. **28**, 1707228 (2018).
[160]V. Magdanz, I. S. M. Khalil, J. Simmchen, G. P. Furtado, S. Mohanty, J. Gebauer, H. Xu, A. Klingner, A. Aziz, M. Medina-Sánchez, O. G. Schmidt, and S. Misra, "IRONSperm: Sperm-templated soft magnetic microrobots," Sci. Adv. **6**, eaba5855 (2020).

Published under an exclusive license by AIP Publishing